Fluorescence Quenching of Pyrene by Copper(II) in Sodium Dodecyl Sulfate Micelles. Effect of Micelle Size As Controlled by Surfactant Concentration

Barney L. Bales*,†

Department of Physics and Astronomy and The Center for Cancer and Developmental Biology, California State University at Northridge, Northridge, California 91330-8268

Mats Almgren‡

Institute of Physical Chemistry, University of Uppsala, S-75121 Uppsala, Sweden

Received: March 27, 1995; In Final Form: June 23, 1995®

The aggregation numbers of sodium dodecyl sulfate (SDS) micelles and the fluorescence quenching constants, k_q, of pyrene by Cu^{2+} have been measured as a function of SDS concentration from 25 to 200 mM. The results confirm an empirical observation made by small angle neutron scattering (Bezzobotnov, et al. *J. Phys. Chem*, **1988**, 92, 5738) that SDS micelles grow linearly as the one-fourth power of the total detergent concentration. The aggregation numbers, computed under the assumption that the Cu^{2+} ions are distributed randomly among the micelles show a positive slope with increasing Cu^{2+} concentration, contrary to theoretical expectations; however, invoking, a small electrostatic repulsion between Cu^{2+} ions residing upon the same micelle brings the experimental observations into agreement with theory. This electrostatic repulsion decreases from $\epsilon_2 = 0.11$ to $0.04kT$ (T = absolute temperature, k = Boltzmann constant) as the micelle size increases from 50 to 85 molecules. These electrostatic repulsion energies are comparable to those necessary to bring electron paramagnetic resonance results into agreement with theory as presented in the following paper. The quenching constant decreases with the size of the micelle according to $k_q = \gamma D/R^2$ with a coefficient of correlation $r = 0.994$, consistent with a model of diffusion encounters between reactants moving on or near a sphere of radius R. D is the relative diffusion coefficient of the reactants and γ is a constant. Taking R to be the radius of the micelle and reasonable estimates of γ shows that the diffusion coefficient of Cu^{2+} is of the same order of magnitude as it is in water. This leads to the conclusion that the quenching rate constant is nearly diffusion controlled and that pyrene is readily available at the micelle surface to participate in molecular collisions with Cu^{2+}. Further, the residence time of the Cu^{2+} upon any given head group must be rather short. Even though the data are better fit under a hypothesis of electrostatic repulsion, the conclusions that the micelles grow as the one-fourth power of the detergent concentration and that the quenching is consistent with a surface diffusion mechanism are unaffected if a random distribution is utilized. Under this latter interpretation, the micelles grow from 57 to 89 molecules as the SDS concentration increases from 25 to 200 mM. The observed micelle growth together with an absence of substantial polydispersity is inconsistent with thermodynamic predictions.

Introduction

One interesting and important aspect of compartmentalized liquids is their ability to concentrate additive molecules into relatively small effective volumes which increases the rate at which such molecules encounter one another.[1−4] In principle, the collision rate between two additive molecules may be studied by monitoring a measurable quantity that is altered during the act of collision. In practice, since the collisions are frequent, a fast measurement technique is needed, and thus far only two have been developed: quenching of fluorescence studied by time-resolved techniques[5−7] and spin-relaxation of stable free radicals studied by EPR.[8−12] Particularly simple is the case in which molecules collide on a much shorter time scale if they occupy the same compartment that they do if they occupy different compartments. Nevertheless, even in this case, the measurement of the bimolecular collision rate is complicated by the fact that a sample contains a statistical distribution of additives among compartments. Thus, the signal is a superposition of signals due to compartments containing zero, one, two, three, etc., additives. Either these component signals must be separated or the superposition must be interpreted under testable assumptions. So far, the separation has been effected in neither the fluorescence nor the EPR experiment; therefore, the superposition must be interpreted, and central to this interpretation is an understanding of the statistics of the distribution of additives. This work is our first effort to measure the fluorescence and the EPR of nearly identical samples and to find a consistent interpretation of the two experiments. The quencher in the fluorescence experiment and the broadener in the EPR experiment is Cu^{2+} derived from the same mother solution. The samples differ in that the hydrophobic probe pyrene is used in the fluorescence experiment and the hydrophobic nitroxide free radical **I** is used in the EPR.

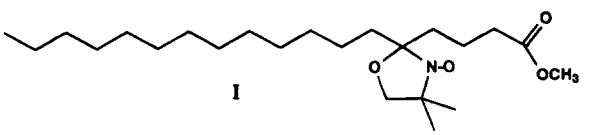

I

The prototype systems in studies of compartmentalized liquids are small, ionic micelles formed by detergents in water at

† E-mail: bbales@huey.csun.edu.
‡ E-mail: almgren@iris6.fki.uu.se.
® Abstract published in *Advance ACS Abstracts,* September 15, 1995.

0022-3654/95/2099-15153$09.00/0

relatively low concentrations.[1-4] Fluorescence quenching techniques have dominated the experimental efforts,[5-7] and the discussion usually begins with the zero-order view of these micelles as being almost spherical and of about the same size. The simplest experiments involve fluorescence probes and quenchers that remain in the same micelle for times much longer than the lifetime of the fluorescence probes. Fluorescence quenching has contributed a great deal to our understanding of the dynamics of additive molecules, while at the same time providing estimates of the sizes of the micelles; however, the additives are almost always assumed to be distributed randomly among identical micelles. This yields the Poisson distribution, which means that there are no interactions between the additive particles.

Recently, one of us has been exploring to what extent EPR could be a useful technique complementary to fluorescence quenching.[9,13] For SDS micelles in the detergent concentration range 25−200 mM, it was not possible to fit the data using Poisson statistics and the best available estimates of the aggregation numbers.[9] Unfortunately, a significant spread in these aggregation numbers reported in the literature, both from technique to technique and using the same technique, complicated the analysis. Further, it could be logically inconsistent to use aggregations numbers derived from a hypothesis of a random distribution to interpret EPR data, which requires a nonrandom distribution, although it is possible that the additives in the EPR experiment and those in the fluorescence experiment distribute differently. This is one of the motivations to use the same additive in both experiments.

From fluorescence data, it was thought[14] that SDS micelles grew as a function of detergent concentration. Small-angle neutron scattering results supported this idea and suggested[15] that this growth was described by $N_A \propto [SDS]^{1/4}$, where N_A is the aggregation number. Empirically, we write

$$N_A = \kappa_1[SDS]^{1/4} \tag{1a}$$

or, alternatively, supposing a nonzero intercept

$$N_A = \kappa_3 + \kappa_2[SDS]^{1/4} \tag{1b}$$

If eq 1a or 1b were accurate, it would give a systematic basis upon which to interpret other data. For example, the average polarity of SDS micelles as sensed by the solubilized free radical **I** was found to vary linearly with $[SDS]^{1/4}$, suggesting that the polarity varies with micelle size.[13] As another example, the quenching rate constants of pyrene with a variety of quenchers is known to decrease with SDS concentration. With a size dependence given by eq 1, a framework is available to test the suggested size variations of the first-order quenching rate constant, k_q. One example is[3, 16]

$$k_q = \gamma_F D/R^2 \tag{2}$$

where R is the radius of the micelle, D is the sum of the translational diffusion coefficients of the probe and the quencher, and γ_F is a constant. The subscript F refers to fluorescence.

The purpose of the present work is 3-fold: first, to carry out a systematic measurement of the aggregation number as a function of [SDS] in order to test eq 1; second, to test eq 2; and third, to provide fluorescence quenching data on the same system which is studied using EPR and reported in the companion paper.[17]

Theory

The time-dependent fluorescence signal following a short pulse at $t = 0$ from immobile probes in the presence of mobile quenchers has been successfully interpreted using the following:[18, 19]

$$f(t) = A_1 \exp\{-A_2 t + A_3[\exp(-A_4 t) - 1]\} \tag{3}$$

where

$$A_1 = f(0) \tag{4}$$

$$A_2 = k_0 + \frac{k_q k_- \langle N\rangle}{(k_q + k_-)} \tag{5}$$

$$A_3 = \frac{\langle N\rangle k_q^{\,2}}{(k_q + k_-)^2} \tag{6}$$

$$A_4 = k_q + k_- \tag{7}$$

where $k_0 = 1/\tau_0$ is the decay rate constant for the pyrene in the absence of quenching, k_q the rate constant of quenching by a single quencher, k_- the exit rate constant of a quencher from a micelle, and $\langle N\rangle$ the average number of quenchers per micelle. See, for example, ref 5 and references therein for details on the assumptions involved in the derivation of eqs 3−7 together with historical perspectives.

One of the assumptions in the derivation of eq 3 is that the quenchers are distributed among the micelles randomly as described by the Poisson distribution

$$P_{\langle N\rangle N} = \frac{\langle N\rangle^N}{N!}\exp(-\langle N\rangle) \tag{8}$$

where $P_{\langle N\rangle N}$ is the probability of finding $N = 0, 1, \ldots$, quenchers on a given micelle in a sample containing an average number of quenchers per micelle $\langle N\rangle$. In the time-resolved fluorescence experiment, under the assumption of the Poisson distribution, $\langle N\rangle$ is derived from the probability of having zero quenchers on a micelle, $N = 0$ as follows:

$$\langle N\rangle_{\text{Poisson}} = -\log(P_{\langle N\rangle 0}) \tag{9}$$

If, in fact the distribution is altered by interactions between quenchers yielding a value of $P_{\langle N\rangle 0}$ different from the Poisson distribution, then eq 9 is incorrect. We derive the first-order correction to $\langle N\rangle$ by assuming that eq 9 gives the corrected $\langle N\rangle$ if the corrected $P_{\langle N\rangle 0}$ is employed, i.e., that the correct average number is still determined by the number of unoccupied micelles. This ought to be an excellent approximation since the determination of $\langle N\rangle$ is dominated by the fit of eq 3 to the experimental data at times long compared with $1/A_4$, at which point the signal due to probes in micelles containing one or more quenchers has decayed.

A method to calculate distribution functions for additive molecules that interact with one another has been derived previously.[9] For a given value of $\langle N\rangle$, $P_{\langle N\rangle N}$ may be calculated from the following:

$$P_{\langle N\rangle N} = \frac{1}{z}\frac{1}{N!}\exp\left(\frac{\mu N - \epsilon_N}{kT}\right) \tag{10}$$

where the one-micelle grand partition function, z, is given by

$$z = \sum_{N=0}^{\infty}\frac{1}{N!}\exp\left(\frac{\mu N - \epsilon_N}{kT}\right) \tag{11}$$

where ϵ_N is the total interaction energy of N quenchers associated

with one micelle, k the Boltzmann constant, and T the absolute temperature. In eqs 10 and 11, μ is the chemical potential per added molecule which must be adjusted to give the correct $\langle N\rangle$, thus,

$$\langle N\rangle = [\text{quenchers}]/[\text{micelles}] = \sum_{N=0}^{\infty} NP_N \qquad (12)$$

where the square brackets denote molar concentrations. The concentration of micelles is

$$[\text{micelles}] = \frac{[\text{surfactant}] - [\text{surfactant}]_f}{N_A} \qquad (13)$$

where [surfactant] and $[\text{surfactant}]_f$ are the molar concentrations of total surfactant and monomeric surfactant, respectively, and N_A is the aggregation number. Defining

$$\eta = \frac{[\text{quenchers}]}{[\text{surfactant}] - [\text{surfactant}]_f} \qquad (14)$$

it follows from eqs 12−14 that

$$\langle N\rangle = \eta N_A \qquad (15)$$

The numerical evaluation of $P_{\langle N\rangle N}$ is discussed in Appendix A of ref 9.

For a discussion of modeling interactions of additive molecules, see ref 9. One such model, electrostatic repulsion, was successful in bringing theory and experiment into agreement in EPR studies of Co^{2+} acting as a broadener of the EPR lines of the nitroxide free radical **I**. In free space, the energy required to form a uniformly charged, thin spherical shell of total charge Nz_Ie and radius R is

$$\epsilon_N = N(N-1)\epsilon_2 \qquad (16)$$

with

$$\epsilon_2 = (z_Ie)^2/8\pi\epsilon_0 R \qquad (17)$$

where z_I is the charge state of the ion, e the charge of an electron, and ϵ_0 the permittivity of free space. Note that the zero of energy in eq 17 is with all quenchers already associated with some micelle. Substituting typical values into eq 17 yields energies much larger than kT, but in the case of a micelle, there would be shielding effects, a different permittivity, and an almost complete compensation of the added charge by exiting counterions[20] so ϵ_2 is treated as an adjustable parameter. Small departures from the Poisson characterized by $\epsilon_2/kT \approx 0.15$ accounted for earlier EPR results[9] on Co^{2+}.

To explore the effect of electrostatic repulsion on fluorescence quenching-derived aggregation numbers, we proceed as follows: for a given value of ϵ_2 and a given (correct) value of $\langle N\rangle$, $P_{\langle N\rangle 0}$ is computed numerically using eqs 10 and 11 and $\langle N\rangle_{\text{Poisson}}$ is calculated from eq 9. Carrying out calculations for $\langle N\rangle = 0-2$ and $\epsilon_2/kT = 0-0.2$, we find that the results are well described by the simple empirical relationship

$$\langle N\rangle_{\text{Poisson}}/\langle N\rangle = 1 + \kappa\langle N\rangle \qquad (18)$$

Thus, the fractional error is linear with $\langle N\rangle$ with a slope of κ which depends on ϵ_2. This dependence, found numerically, is well approximated as follows:

$$\epsilon_2/kT = \kappa[1 + {}^1/_2\kappa] \qquad (19)$$

TABLE 1: SDS Sources and Treatments

source	treatment	cmc,[b] mM
Kodak Lot No. C15F (**SDS1**)[a]	recrystallized from 95% ethanol, rinsed with ethanol and anhydrous ether at 0 °C, dried under vacuum for 10 days	8.3 ± 0.3
BDH specially pure Lot No. 6779090K (**SDS2**)	as received; stored in desiccator	8.3 ± 0.2
Sigma, Lot No. 46F-0543 (**SDS3**)	as received; capped, but no other precautions in storing	8.1 ± 0.2

[a] The three sources of SDS are designated **SDS1**, **SDS2**, and **SDS3** in the text. [b] Surface tension measurements using the drop volume method. The errors are the estimated uncertainties in locating the intersections of the tangents to the experimental curves above and below the cmc.

Over the ranges $\langle N\rangle = 0-2$ and $\epsilon_2/kT = 0-0.2$ the linearity of eq 18 is excellent, with a squared coefficient of correlation $r^2 > 0.999$, while eq 19 yields the correct value of ϵ_2/kT to within 2%. [We have not managed to sum eq 11 analytically using eq 16; however, the simplicity of eqs 18 and 19 suggests that it could be summed.] Utilizing eq 15, eq 18, may be written

$$N_A(\text{Poisson}) = N_A^0 + \kappa(N_A^0)^2\eta \qquad (20)$$

where $N_A(\text{Poisson}) = \langle N\rangle_{\text{Poisson}}/\eta$ is the apparent aggregation number from fluorescence quenching experiments under the assumption of the Poisson distribution of quenchers and the superscript zero is a reminder that N_A^0 is the proper aggregation number evaluated in the limit of small η. Thus, if small electrostatic repulsion between quenchers alters the distribution, eq 20 shows that a plot of $N_A(\text{Poisson})$ vs η ought to be linear with a slope of

$$\frac{\partial N_A(\text{Poisson})}{\partial\eta} = \kappa(N_A^0)^2 \qquad (21)$$

and an intercept of N_A^0. The experimental data are treated as follows: $N_A(\text{Poisson})$ is plotted vs η and fit to a straight line. The intercept of the line gives N_A^0 while the slope yields ϵ_2/kT using eqs 21 and 19.

Materials and Methods

Reported aggregation numbers for SDS micelles are quite scattered.[7] One concern is the purity of the detergent, thus we have used three sources as outlined in Table 1. The surface tensions of SDS from these three sources were measured using the Lund surface tension apparatus operating on the drop volume principle.[21] Solutions near 25 mM were prepared and allowed to age from 1 h to overnight. The rest of the series was then prepared by dilution with deionized water, the concentrations being determined gravimetrically. All samples were at least 4 but less than 30 h old when the surface tension measurements were made. Generally 5−6 measurements of the number of counts per drop of solution were made, being increased to 8−9 at concentrations near the cmc from which the surface tensions were computed using correction factors given by Wilkinson.[22] Figure 1 shows the results, which compare well with curves in the literature.[23] The standard deviations are smaller than the plot symbols and no minimum is detectable in any of the three SDS sources. The cmc's of each detergent, estimated by finding the intersection of the tangents to the experimental curves above and below the break points in the curves, are given in Table 1. The quoted errors are the estimated uncertainties in locating these intersections. **SDS3** shows a marginally reduced cmc and, as Table 3 shows below, a marginally increased aggregation number compared with the other sample sources; however, these

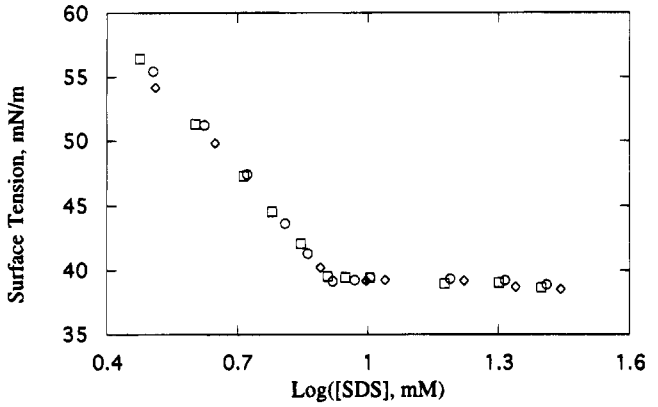

Figure 1. Surface tension vs detergent concentration for three sources of sodium dodecyl sulfate, **SDS1** (○); **SDS2** (◇); **SDS3** (□), determined by the drop method at room temperature.

differences are not significantly larger than the experimental uncertainties. There are numerous literature values of the cmc for SDS: examples are cmc = 7.6,[23] 8.1,[1] and 8.2 mM.[24]

Anhydrous copper sulfate (Fluka) heated in an oven at 160 °C overnight showed no weight loss. A 63.9 mM stock solution in water was prepared by weight to a precision of 0.1% and stored in a tightly capped vial. An atomic absorption measurement yielded a concentration that was 6% larger than the gravimetric value. Had the gravimetric value been the larger of the two, this would have suggested that the $CuSO_4$ could have been contaminated with a small amount of $CuSO_4 \cdot H_2O$; however, as it is, we are at a loss to explain the discrepancy. We report the results using the gravimetric measurements and note that the absolute values of N_A would be systematically smaller by 6% if the atomic absorption concentrations were used. The relative precision of values of N_A are unaffected by this uncertainty. Typically, 0.3-g aliquots of the stock $CuSO_4$ solution were transferred to vials and evaporated in an oven overnight, cooled, capped, and stored for later use. Special care was taken to transfer the solution to the bottom of the vials and to handle them carefully to minimize the possibility of leaving undissolved $CuSO_4$ in the vial during sample preparation.

A stock 5.00 mM solution of pyrene (Aldrich, recrystallized twice from spectroscopic grade ethanol) was prepared in spectroscopic grade ethanol and stored in the dark in a tightly stoppered vial covered with a plastic film. Stock pyrene solution, typically 100 μL, was transferred to vials, the solvent removed with a stream of dry, pure nitrogen gas, capped, and stored in the dark for later use.

Experiments were carried out using the three sources of SDS one at a time. Typically, 2 days before the fluorescence quenching experiment, an SDS solution near 200 mM solution was prepared gravimetrically to a precision of better than 0.1%. [The density of SDS solutions as determined by Mr. Göran Svensk using a Paar density meter DMA60, varies linearly from 998.1 kg/m^3 for [SDS] = 25 mM to 1005.0 kg/m3 for [SDS] = 200 mM, thus conversion to the molarity scale requires corrections of less than 0.5%.] After stirring the SDS gently for about 1 h, a weighed quantity was added to a vial containing pyrene to yield a pyrene:SDS molar ratio of 1:300 ± 10% and stirred overnight. Excimer formation was found to be negligible as judged by static fluorescence emission measurements. Pyrene/SDS solution was added gravimetrically to a vial containing $CuSO_4$ to give a molar ratio $CuSO_4$:SDS near 1:25 to a precision of 0.2% and stirred for 1 h. Solutions at lower $CuSO_4$:SDS ratios were prepared gravimetrically by mixing the SDS/pyrene solution with the SDS/pyrene/Cu^{2+} solution. These samples, the mother samples, have accurately the same pyrene

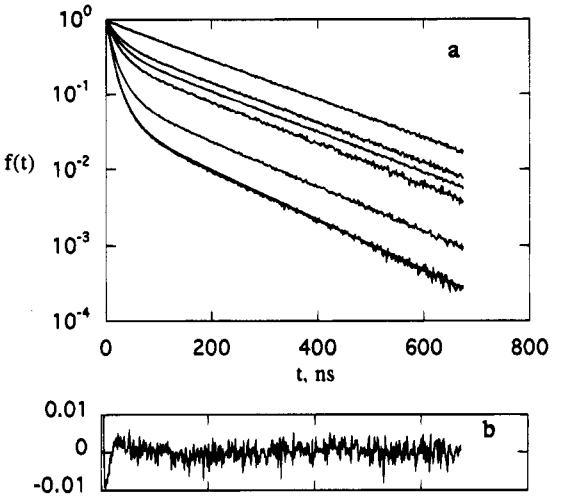

Figure 2. (a) Typical decay curves for pyrene in 50 mM **SDS2** at 25 °C with various concentrations of the quencher Cu^{2+} from the top curve to the bottom as follows: η = 0, 0.0103, 0.0140, 0.0179, 0.0346, and 0.0463. The bottom curve, at η = 0.0463 has the least-squares fit of eq 3, employing Poisson weighting, superimposed upon it. The curves have been normalized to unity. The total number of counts in the zero channel for the curves from top to bottom are as follows: 3.42×10^4, 2.09×10^5, 1.90×10^5, 3.25×10^4, 2.09×10^5, and 2.26×10^5. The almost parallel long-time tails of the curves are characteristic of small migration rates of Cu^{2+} from the micelles. (b) The residuals from the fit of the η = 0.0463 curve showing some autocorrelation near the origin. At lower values of η the residuals are similar to those in Figure 3.

concentrations and $CuSO_4$:SDS ratios known to a relative precision of 0.2% assuming that all of the $CuSO_4$ is dissolved. After mixing the mother samples by gently rocking and swirling, samples at lower values of [SDS] were prepared gravimetrically by dilution with water. This method of preparation preserves the $CuSO_4$:SDS ratios as well as the pyrene:SDS ratios as η is reduced. These samples were mixed by gently rocking and swirling and, after sitting overnight in the dark, were transferred to cuvettes for the fluorescence measurements. Thus typically, samples were measured about 2 days after the SDS was first prepared and 1 day after the $CuSO_4$ was added; however, these times varied by as much as 1 day. Time-dependent effects have not been studied, but they appear to be small as far as N_A and k_q are concerned since these quantities are well reproduced from experiment to experiment. The electrostatic repulsion, ϵ_2/kT, is not as well reproduced, and it is unknown if this is due to small time-dependent effects or other random errors.

Fluorescence decay data were accumulated using the time-correlated single-photon-counting technique using a mode-locked Nd:YAG laser (Spectra Physics 3800/451) pumping a cavity-dumped DCM-dye laser (Spectra Physics 3500/454). The photon frequency was tuned and frequency doubled with a KDP crystal to excite pyrene at 318 nm. The pyrene monomer emission was detected at 393 nm by a Tennelec TC952 photomultiplier and converted to the time domain with a CDF, Schlumberger 7174 and a TAC Tennelec TC 862 and collected with an IBM PS2. For further details see refs 25 and 26.

Static fluorescence spectra were obtained with a Spex Fluorolog 1680 with a Spex Spectroscopic Coordinator DM1B with a dispersion 1.8 nm/mm.

Results

Figures 2 and 3 respectively show fluorescence decay curves for pyrene in 50 mM **SDS2** and 200 mM **SDS1** in the presence of various concentrations of Cu^{2+}. These are typical of all the curves measured and are well described by eq 3. Fits to eq 3,

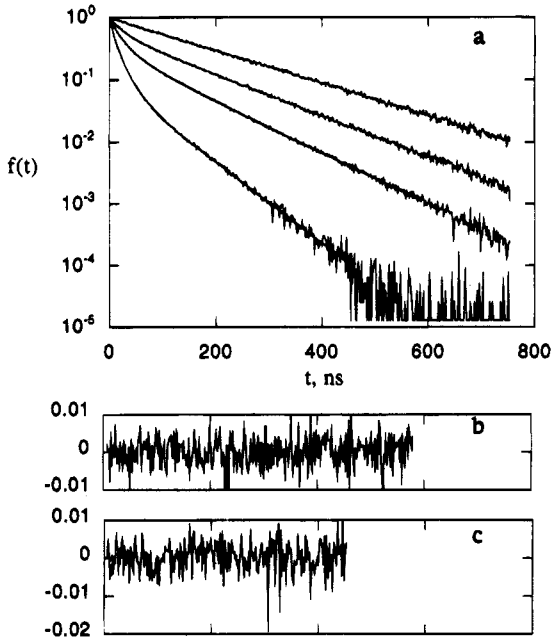

Figure 3. (a) Typical decay curves for pyrene in 200 mM **SDS1** at 25 °C with various concentrations of the quencher Cu^{2+} from the top to the bottom curve as follows: $\eta = 0$, 0.00818, 0.0163, and 0.0326. The bottom two curves, at $\eta = 0.0179$ and 0.0346, respectively, have the least-squares fits of eq 3, employing Poisson weighting, superimposed upon them. The curves have been normalized to unity. The total number of counts in the zero channel for the curves from top to bottom are as follows: 2.20×10^4, 1.87×10^4, 6.40×10^4, and 7.53×10^4. The increasing slopes of the long-time tails of the curves from top to bottom are characteristic of migration rates, k_- that are comparable with the decay rates of pyrene. (b) The residuals from the fit of the $\eta = 0.0163$ curve and (c) from the $\eta = .0.0326$ curve.

using Poisson weighting of the data, were carried out using the Levenberg–Marquardt algorithm yielding parameters A_j, $j = 1-4$. In all cases, except for the noise, the curves describing the fits are practically indistinguishable from the data. The residuals are generally small and random except for quite high values of η. In 50 mM SDS, some autocorrelation in the residuals is evident at $\eta = 0.0463$. The, almost parallel long-time tails in the decay curves for 50 mM SDS (Figure 2) are indicative of immobile quenchers, i.e., small values k_-, while nonnegligible migration is evident in the curves corresponding to 200 mM SDS (Figure 3). Parameters $\langle N \rangle$, k_q, and k_- were determined from eqs 29–31 and the aggregation number, N_A-(Poisson) was calculated from eq 15. Estimates of the uncertainties in these quantities were derived as described in Appendix A.

Aggregation Numbers. Figure 4 shows the apparent aggregation number of SDS micelles as a function of η for four concentrations of the purified SDS, **SDS1**. To compute η, the values of $[SDS]_f$ given in Table 2 were employed.[23,27] The error bars are computed from the uncertainties in the fitting parameters according to eq 32. The aggregation numbers are computed from the experimental data assuming the Poisson distribution which predicts that the curves in Figure 4 would be straight horizontal lines, and indeed such lines would fall nearly within the experimental uncertainty of the results. Nevertheless there seems to be a positive slope to the data in Figure 4 and such a positive slope was found, with a single exception, in experiments at all SDS concentrations and using the three different sources of the detergent. A negative slope in such plots can be an indication of micelle size polydispersity and can be used to estimate its magnitude (ref 28 and references therein). In the case of SDS, the effect would be very small.[29] A positive slope

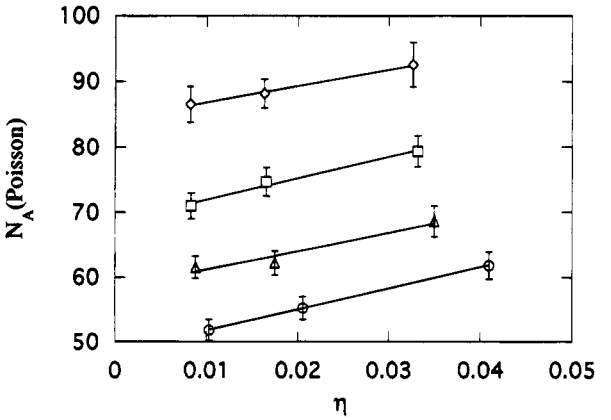

Figure 4. Aggregation numbers of micelles at 25 °C from the purified source of sodium dodecyl sulfate, **SDS1**, derived from the fluorescence quenching of pyrene by Cu^{2+}. The curves from bottom to top correspond to detergent concentrations of 25, 50, 100, and 200 mM, respectively. The aggregation numbers are computed under the assumption of a Poisson distribution of the Cu^{2+} ions using the fit of the decay curves to eq 3 and eqs 29 and 15 and the error bars are computed from eq 35. The straight lines are least-squares fits to eq 20 yielding the values of the electrostatic repulsion energies ϵ_2 listed in Table 2. The squared coefficients of correlation for the fits from bottom to top are as follows: $r^2 = 0.999$, 0.942, 0.994, and 0.985.

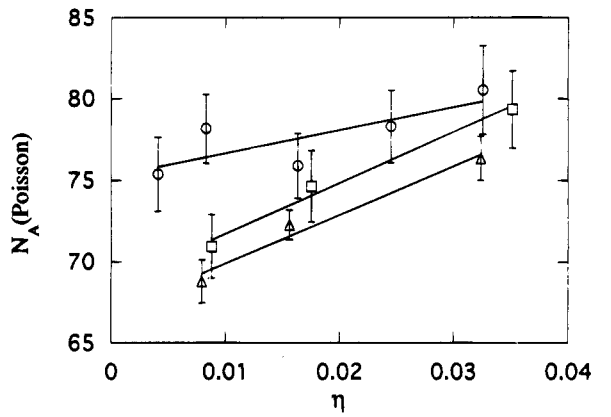

Figure 5. Aggregation numbers of micelles at 25 °C of 100 mM sodium dodecyl sulfate from three sources, **SDS1** (○); **SDS2** (△); **SDS3** (□). The calculations and error bars are the same as in Figure 4.

TABLE 2: Values of Repulsion Energy ϵ_2/kT for Cu^{2+} in SDS Micelles ($T = 25$ °C)

[SDS], mM	$[SDS]_f$, mM	SDS1	SDS2	SDS3	mean
25	5.3	0.15	0.08		0.11 ± 0.05
50	3.8	0.09	0		0.04 ± 0.06
100	2.5	0.07	0.07	0.025	0.06 ± 0.03
200	1.7	0.04	0.04		0.04

could be explained by a slight departure from the Poisson distribution caused by small effective electrostatic interactions between Cu^{2+} ions residing on the same micelle. The lines in Figure 4 are plots of eq 20 using the values of ϵ_2/kT given in Table 2 which also lists the mean values of ϵ_2/kT for all sources of SDS at various detergent concentrations. It is noted that these values of ϵ_2/kT are of the same order of magnitude as those previously found in EPR experiments using cobalt(II)[9] and in the companion paper using copper(II);[17] however, as Table 2 shows, they are not well reproduced.

Figure 5 gives an idea of the variation of the computed aggregation number from one SDS source to another as a function of the quencher concentration for [SDS] = 100 mM. The straight lines are plots of eq 20 using values of ϵ_2/kT given in Table 2. The intercepts of these plots have been averaged over different SDS sources and the mean values and standard

TABLE 3: Values of the Aggregation Number N_A for SDS Micelles (T = 25 °C)

[SDS], mM	N_A(Poisson) SDS1[a]	SDS2[a]	SDS3[a]	mean[b]	N_A^{0}[c] repulsion
25	56.2 ± 4.8	58.8 ± 2.7		57.3 ± 3.9	50.7 ± 3.0
50	64.1 ± 3.6	70.0 ± 1.6		68.3± 3.4	64.4 ± 8.1
100	75.0 ± 4.0	72.5 ± 3.5	77.7 ± 2.0	75.5 ± 3.4	70.2 ± 4.1
200	89.0 ± 3.0	89.1 ± 2.1		89.1 ± 2.3	84.9 ± 0.8

[a] Average over all values of η; errors are standard deviations. [b] Average of columns 2−4; errors are standard deviations. [c] Average of the intercepts in the fits to eq 20; errors are standard deviations.

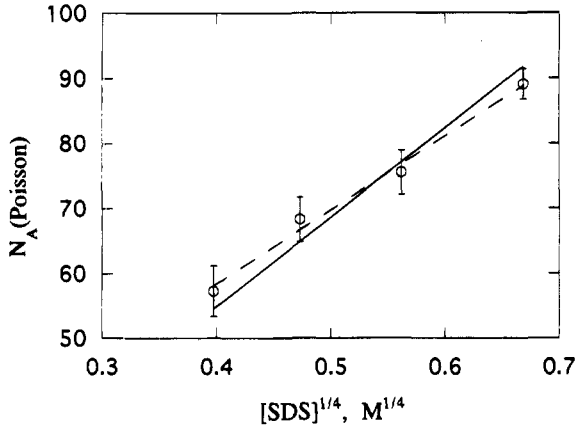

Figure 6. Variation of aggregation numbers with [SDS]$^{1/4}$ at 25 °C. Each point is the unweighted average of results at all values of η and all sources of sodium dodecyl sulfate (column 5 of Table 3). The error bars are standard deviations. This treatment of the data assumes the Poisson distribution of Cu^{2+} ions and includes the slopes of curves such as those in Figures 4 and 5 as sources of error. The solid line is a least-squares fit of the data to eq 1a and the dashed to eq 1b. See text for the fit parameters and correlation coefficients.

deviations are given in the final column of Table 3. Since, within the precision of the present experiments the variation of N_A(Poisson) with η and from SDS source to source is of the same order of magnitude as the uncertainties, we have averaged the results at all values of η and reported the mean values and standard deviations in columns 2−4 of Table 3. Column 5 is the average of columns 2−4. Thus the final two columns of Table 3 report aggregation numbers under a hypothesis of electrostatic repulsion (column 6) and random distribution (column 5).

To evaluate the precision of eqs 1a and 1b, the data in column 5 of Table 3 are plotted vs [SDS]$^{1/4}$ in Figure 6. The solid line is a linear least-squares fit of the data to eq 1a with κ_1 = 137 molecules/M$^{1/4}$ and a squared coefficient of correlation r^2 = 0.947 while the dashed line is a similar fit to eq 1b with κ_2 = 114 molecules/$M^{1/4}$, κ_3 = 13 molecules, and r^2 = 0.990. Either eq 1a or 1b falls within experimental error of the data; however, the fit is better with eq 1b. A plot of the data of column 6 of Table 3 (not shown), derived under an assumption of electrostatic repulsion between the Cu^{2+} ions, is similar to Figure 5, with fits to either eq 1a or 1b passing within experimental error of the data. These fits yield the following parameters: κ_1 = 128 molecules/$M^{1/4}$ and r^2 = 0.968 for eq 1a and κ_2 = 120 molecules/$M^{1/4}$, κ_3 = 5 molecules, and r^2 = 0.974 for eq 1b.

Assessing the accuracy of eq 1a or 1b by using the data of Table 3 involves the uncertainty as to the origin of the variation of N_A(Poisson) with η. By studying the variation of N_A(Poisson) with [SDS] at similar values of η, this uncertainty may be minimized and attention focused upon the effect of [SDS]. For example, Figure 7 shows N_A(Poisson) derived from samples at maximum η plotted vs [SDS]$^{1/4}$. The error bars are the standard

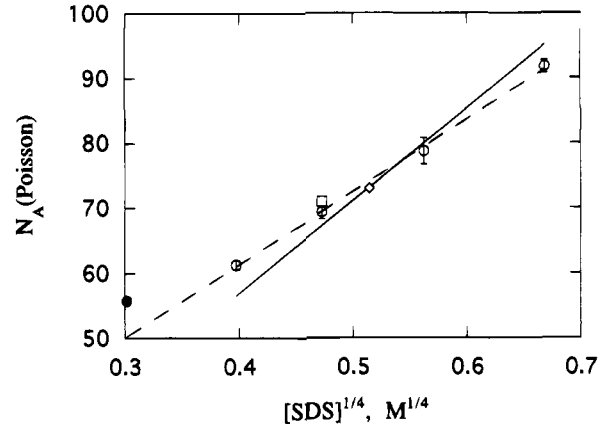

Figure 7. Variation of aggregation numbers with [SDS]$^{1/4}$ at 25 °C (○). Each point is the unweighted average of results from all sources of sodium dodecyl sulfate at values of η near 0.035 (0.033−0.041), and the error bars are standard deviations. This treatment of the data minimizes the uncertainty due to slopes of curves such as those in Figures 4 and 5. The solid line is a least-squares fit of the data to eq 1a, and the dashed line to eq 1b. See text for the fit parameters and correlation coefficients. Two recent literature values from fluorescence quenching data fit to eq 3 are given by (□)[30] and (◇).[29] The light scattering result of Huisman[37] at the cmc, corrected to 25 °C using the data of ref 15 is shown by (●).

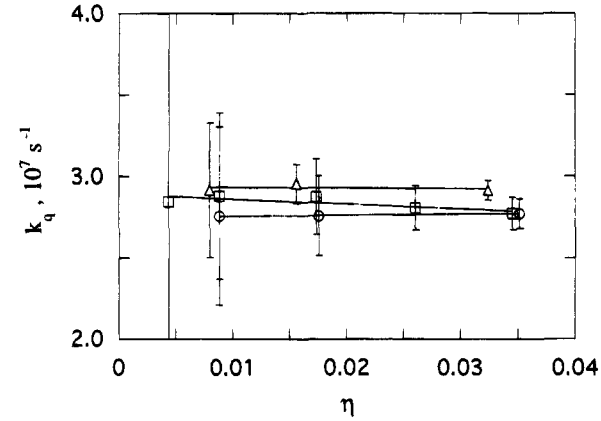

Figure 8. Quenching rate constant vs quencher concentration at 25 °C in 100 mM sodium dodecyl sulfate from three sources, **SDS1** (○); **SDS2** (△); **SDS3** (□). The rate constants are calculated from eq 29 using parameters from the fits of decay curves to eq 3 and thus assume the Poisson distribution of quenchers. The straight lines are linear least-squares fit to the data and the error bars are computed from eq 33.

deviations in the results from two sources of SDS at [SDS] = 25, 50, and 200 mM and from three sources at [SDS] = 100 mM. Linear fits yield the following parameters: κ_1 = 134 molecules/$M^{1/4}$ and r^2 = 0.920 for eq 1a and κ_2 = 105 molecules/$M^{1/4}$, κ_3 = 16 molecules, and r^2 = 0.998 for eq 1b. Equation 1a does not fit the data within experimental uncertainty; however, eq 1b is a remarkably precise description of the micelle size variation with SDS concentration. Included in Figure 7 are two recent aggregation number determinations based upon eq 3 taken from the literature.[29,30]

Quenching Rate Constants. Within experimental error, the rate constant, k_q, is independent of both Cu^{2+} concentration and SDS source. For example, Figure 8 shows a plot of k_q vs η for [SDS] = 100 mM. The error bars are estimated errors computed from eq 33 and the three lines are linear least-squares fits to the data for **SDS1**, **SDS2**, and **SDS3** respectively. Apparently, k_q is significantly more reproducible than the error estimates. Mean values of k_q and standard deviations computed from measurements at all η using all sources of SDS are given in Table 4. These values compare well with literature values in

TABLE 4: Quenching and Escape Rate Constants for Cu^{2+} in SDS[a] (T = 25 °C)

[SDS], mM	k_q, 10^6 s^{-1}	$k_-(0)$, 10^6 s^{-1}	$\partial k_-/\partial\eta$, 10^6 s^{-1}
25	34.9 ± 0.6 (6)	0.07 ± 0.17	4.2 ± 4.1
50	32.1 ± 0.7 (12)	0.21 ± 0.02	5.4 ± 1.9
100	28.4 ± 0.7 (11)	0.70 ± 0.06	8.4 ± 2.5
200	24.9 ± 0.9 (7)	2.25 ± 0.01	28.3 ± 5.9

[a] Mean values and standard deviations from measurements at all η and all sources of SDS. The numbers in the parentheses indicate the number of measurements.

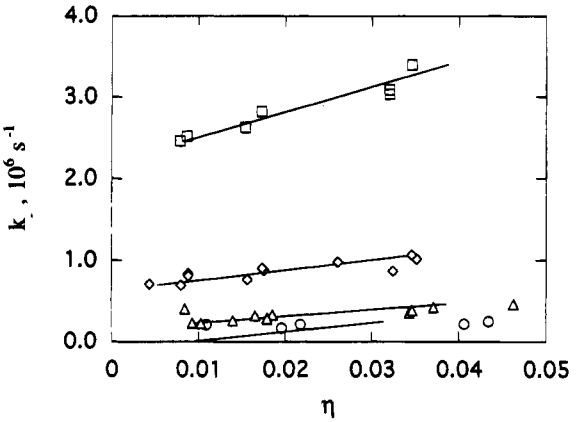

Figure 9. The migration rate constants, k_-, of Cu^{2+}, vs Cu^{2+} concentration from all sources of SDS at 25 °C. The detergent concentrations for the curves from bottom to top are 25, 50, 100, and 200 mM. The straight lines are linear least-squares fits to the data.

some cases[5,31] and poorly in others;[32,33] however, in these latter cases different models were used.

Figure 9 shows that k_- depends on SDS concentration as expected and that a small dependence on Cu^{2+} concentration may be detected as well. Fitting the latter dependence to

$$k_-(\eta) = k_-(0) + \frac{\partial k_-}{\partial \eta}\eta \qquad (22)$$

for each [SDS] and each source of SDS and averaging the intercept and slope gives the results in Table 4. From these data, we find $\ln[k_-(0)] = 17.3 + 1.68 \ln[\text{SDS}]$ with a squared coefficient of correlation $r^2 = 0.9999$.

Since SDS micelles grow as a function of detergent concentration, we may explore the dependence of the rate constant k_q on micelle size. The size dependence has been investigated[34,35] previously using added salt to vary the micelle size, which is worrisome because both shape changes and sizable ionic strength variations might give unpredictable results. The size and ionic strength are varied more modestly in the present experiments, and according to small-angle neutron scattering results,[15] the shape also varies modestly. Supposing that the micelles are approximately spherical allows us to write the micelle volume, V, as follows:

$$V = (4\pi/3)R^3 = N_A V' \qquad (23)$$

where V' is the effective volume per SDS molecule in the micelle. Equation 23 assumes that V' is independent of N_A. Combining eqs 1a and 23, eq 2 may be written

$$k_q = \gamma_F D(4\pi/3V'\kappa_1)^{2/3}[\text{SDS}]^{-1/6} \qquad (24)$$

Figure 10 shows the least-squares fit of k_q to eq 24. The slope

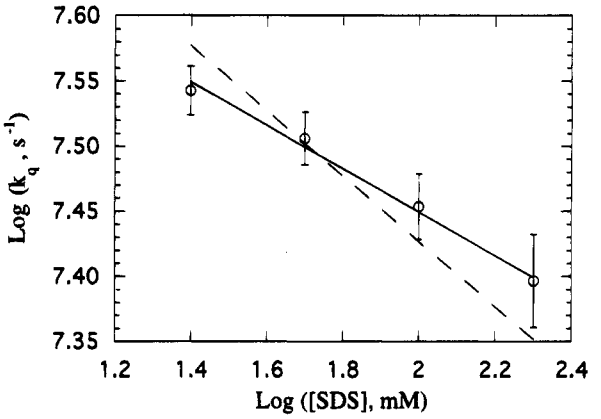

Figure 10. Quenching rate constant vs SDS concentration at 25 °C. The points are unweighted average of results at all values of η, and all sources of sodium dodecyl sulfate and the error bars are standard deviations. The solid line is a linear least-squares fit of the data to eq 24 corresponding to a surface diffusion model, eq 2, and a micelle growth given by eq 1a. The dashed line is the best fit to k_{2q}/V, where V is the micelle volume.

of this fit yields

$$\gamma_F D(4\pi/3V'\kappa_1)^{2/3} = (1.92 \pm 0.01) \times 10^7\ M^{1/6}\ s^{-1} \qquad (25)$$

where the correlation coefficient, $r = 0.994$. Using R = 20 Å at $N_A = 62^{27}$ yields $V' = 5.40 \times 10^{-28}$ m^3 and by supposing κ_1 = 142 molecules/$M^{1/4}$, we find that $\gamma_F D \approx 1.3 \times 10^{-10}$ m^2/s.

The fit of the data is satisfacory using the 2-dimensional diffusion model of eq 2. For comparison, the best fit of the data to an equation of the form $k_q = k_{2q}/V$, where V is the micelle volume and k_{2q} is a constant, appropriate for a 3-dimensional diffusional model, is indicated by the dashed line in Figure 10 which is clearly an inferior fit.

Discussion

High-precision absolute determination of micelle sizes at detergent concentrations above the cmc continues to be a problem. Even the size determination using the same time-resolved fluorescence quenching data depends upon the data reduction technique. For example, in a recent, careful study of 70 mM SDS in the absence of salt, Siemiarczuk et al.[29] found an aggregation number of 72.6 ± 1.3 using fits to eq 3 and 62 ± 3 from a graphical analysis. These are micelles that show very little size dispersion,[29] so that complication cannot be the source of the discrepancy. Interpretation of small-angle neutron scattering data is complicated by the need to normalize the scattering intensity data and uncertainty about the interparticle structure factor $S(Q)$.[15] In view of these problems, it is not surprising that careful review of micelle sizes shows a rather large spread. For example, see Figure 4 of ref 9.

It appears that *relative* micelle sizes may be determined with good precision if the technique and the data reduction are consistently applied to samples not prone to systematic errors. In this work, the rather small error bars in Figure 7 are standard deviations in measurements using different sources of SDS. These uncertainties do not reflect the uncertainty in $[Cu^{2+}]$; however, since all the samples, as well as all of those in the companion EPR paper,[17] are traced to the same mother solution the *relative* values of η are precise. Neither do the uncertainties of Figure 7 reflect, to a large extent, the uncertainty introduced by the slopes of the curves in Figures 4 and 5 since they are derived from measurements at similar values of η. In view of

these observations, the difference in the aggregation numbers derived from the Poisson distribution (column 5 of Table 3) and those derived from a distribution altered slightly by electrostatic repulsion between copper ions (column 6 of Table 3), while important and interesting theoretically, are not very significant practically.

Empirically, the sizes of SDS micelles are very well described by eq 1b, especially if precautions discussed in the previous paragraph are observed when exploring the size variation with detergent concentration. Two recent measurements,[29,30] both interpreted using eq 3, were added to Figure 7 for comparison and the time-honored datum[36] of Huisman[37] at the cmc is included as well. As far as we know, there is no compelling theoretical reason to expect SDS micelles to grow as $[SDS]^{1/4}$, although Bezzobotnov et al.[15] have offered some insights. Given the precision of the empirical description, pursuit of a deeper theoretical understanding seems to be worth while. Also worthwhile, would be systematic measurements such as these in other detergent systems.

Table 2 results from an interpretation of curves such as those in Figure 4 in terms of a small electrostatic repulsion between the cationic quenchers. That the results are not better reproduced is worrisome. Indeed, if it were not for the fact that such repulsions bring experiment and theory into agreement in EPR experiments,[9,17] such an interpretation for these results would be suspect. Our original goal in undertaking simultaneous fluorescence and EPR experiments was to determine, with precision, the micelle sizes using fluorescence and interpret the EPR with those sizes fixed. If interpretation of the EPR were to require a nonrandom distribution, then we would redetermine the micelle sizes from the fluorescence data using the same altered distribution. A few iterations of the size vs distribution adjustment cycle were envisioned to be necessary to reach a consistent treatment. We have not succeeded in this goal, because precise sizes are difficult to obtain as discussed above. At present, the best we can do is to show that the EPR results give repulsion energies of the same order as Table 2 if micelle sizes vary as eq 1b and are near the values given in Figures 6 or 7. At least, the *relative* sizes of micelles as a function of detergent concentration in SDS are now firmly established which is a step toward enabling a global fitting of the two experiments.

Electrostatic repulsion energies in the range $\epsilon_2/kT = 0-0.15$, corresponding to $\epsilon_2 \approx 0-4$ mV represents about 0−3% of the potential (140 mV) of the SDS micelle surface,[7] i.e., a rather small perturbation. See Figure 2 of ref 9 for a plot of the resulting altered statistical distribution compared with the Poisson. If we imagine that as one Cu^{2+} ion is added to the micelle surface, an average of slightly less than two Na^+ ions exit, then the next Cu^{2+} would face an effective repulsion compared with a micelle containing no Cu^{2+} ions. The potential is still attractive, but less so than a micelle not already containing a Cu^{2+}. Miller has discussed such an effect.[20] [In previous work,[9] it was erroneously remarked that electrostatic repulsion would lead to smaller than correct sizes in the fluorescence quenching experiment, when the opposite is the case.]

The quenching rate constants k_q have been derived using eq 3 assuming a Poisson distribution of the quenchers. The values of these rate constants likely depend upon the quencher distribution assumed, but this problem has not been solved for the electrostatic repulsion distribution, so perhaps their absolute values are in error. If we suppose that their relative values are valid, then Figure 10 supports a 2-dimensional diffusion mechanism for the quencher−probe encounters. Tachiya[3] has given a treatment of surface reactions on a sphere. As a rough approximation, his expression for γ_F reduces to $1/\gamma_F = 0.2 + 2.08 \ln(R/d)$ for $R/d > 3$ where R is the radius of the sphere and d is the reaction distance between the centers of reacting molecules. For $d/2R = 0.2$, $1/\gamma_F = 2.2$, and for $d/2R = 0.05$, $1/\gamma_F = 5$. If we take $1/\gamma_F = 4$ and untilize the above estimated value of $\gamma_F D = 1.3 \times 10^{-10}$ m²/s, then $D \approx 5 \times 10^{-10}$ m²/s, very nearly the value for the diffusion coefficient for Cu^{2+} in pure water at 25 °C.[27] This estimate could be in error by as much as 40% depending upon the parameters employed; however, it seems clear that Cu^{2+} diffuses rather freely about the surface of the micelle lingering very little at the point of contact with the micelle surface. In this discussion, we have implicitly assumed that the viscosity is independent of the size of the micelles and, therefore, the diffusion coefficient is a constant. Recalling that the Smolukhovsky equation involves the sum of the coefficients of diffusion of the two particles and that the microviscosity of the environment of **I** increases by about 40% as the SDS concentration increases from 25 to 200 mM, then this assumption is not strictly correct; however, since pyrene is a large molecule, its coefficient of diffusion is probably negligible compared with that of Cu^{2+} and does not contribute significantly to the quenching rate even at the lowest viscosity.

We now turn to a discussion of the implication that the observed rather rapid growth of the aggregation numbers with detergent concentration is expected to have on the polydispersity. It has been thought that there is a connection between the tendency of micelles to change size and their size polydispersity and the general relationships were elucidated for *nonionic* micelles long ago.[38] Recently, Nagarajan[39] drew attention to the fact that Hall, in his general treatment of the thermodynamics of solutions of polyelectrolytes, ionic surfactants, and other charged colloidal systems[38] showed by seemingly compelling thermodynamic arguments, how the average aggregation number, and the average effective degree of counterion dissociation are related to the concentration of micellized surfactant and of added salt. Using some simplifications, Nagarajan[39] derived the following relationship:

$$\mathrm{d} \ln N_{Aw} = [N_{Az}/N_{Aw} - 1]\, \mathrm{d} \ln(\sum N_A X_{N_A}) + N_{Az}(\beta_w - \beta_z)\, \mathrm{d} \ln X_c \quad (26)$$

where X_{N_A} is the concentration of micelles with aggregation number N_A and X_c the total concentration of counterions, including the counterions from singly dispersed surfactants, micelles, and added electrolytes. β is the effective degree of dissociation. Subscripts w and z stand for weight and z averages, respectively:

$$N_{Aw} = \sum N_A X_{N_A} / \sum X_{N_A}$$

$$N_{Az} = \sum (N_A)^2 X_{N_A} / \sum N_A X_{N_A}$$

If the average degree of dissociation varies little with the aggregation number of the micelles, the two averages of β would be the same, and the last term in eq 26 would be zero. The empirical observation that N_{Aw} depends linearly on the surfactant concentration to power $^1/_4$, implies that

$$(\sigma/N_{Aw})^2 = N_{Az}/N_{Aw} - 1 = {}^1/_4 \quad (27)$$

when the last term in eq 26 is zero, where σ is the standard deviation of the weight distribution. From the results in Figure 7, we conclude that σ varies between approximately 25 at the lowest and 42 at the highest surfactant concentrations, which

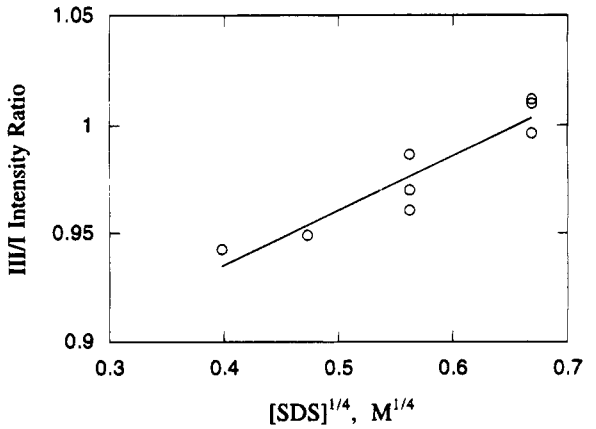

Figure 11. Intensity ratio of the third vibronic band to the first as a function of $[SDS]^{1/4}$. The line is a linear least-squares fit to the data. The increase in III/I is interpreted as a decrease in the average polarity sensed by the pyrene as the micelles grow.

are rather large values. When the polydispersity effect on the time-resolved fluorescence quenching aggregation numbers are explored,[6] the apparent aggregation numbers, $N_A(\eta)$, are found to depend upon the quencher concentration according to

$$N_A(\eta) = N_{Aw} - {}^1/_2\sigma^2\eta \tag{28}$$

where Nagarajan's[39] notation is retained. If there were no direct or indirect quencher interactions, the apparent aggregation number would thus have been expected to decrease rather rapidly with η in Figure 4 instead of the observed increase. This decrease would amount to 13 molecules at [SDS] = 25 mM and 24 molecules at [SDS] = 200 mM. One might argue that the polydispersity effect is concealed by a much larger effect from the repulsive interactions between the quenchers. Contrary to this supposition, however, is the fact that the repulsive energies computed from eq 19 leading to the straight lines in Figure 4 are about the same as those estimated from the EPR measurements in the companion paper.[17] Furthermore, other independent measurements also indicate a low polydispersity for SDS micelles. SANS studies and fluorescence determinations, as well as estimates from the study of micelle kinetics[29,40] all point in this direction. At the same time, however, the strong dependence of the micellar aggregation number on surfactant concentration as well as salt concentration has also been observed in many independent investigations. The inconsistency of these observations with the prediction from the thermodynamic treatment calls for a critical reevaluation of the matter. Even though each experimental datum could be criticized, the fact that several investigations give similar results is a strong argument for their reliability. The generality of the thermodynamic predictions are only achieved through the use of rather heavy formalisms which might conceal flaws in the treatments.

Recently it was reported[13] that the hyperfine coupling constant of **I** varied linearly with $[SDS]^{1/4}$. It is well-known that the hyperfine coupling constant of a nitroxide free radical varies with solvent polarity,[41,42] thus it was suggested[13] that the average polarity sensed by the hydrophobic molecule **I** decreased with increasing micelle size. A detailed model has not been offered, and no other data are yet available, so it would be premature to discuss probe-sensed polarity vs micelle size; however, a brief experiment was carried out in which the steady-state fluorescence emission of pyrene was measured as a function of [SDS]. The intensity ratio of the first vibronic band to the third, the III/I ratio, which is known to increase with decreasing polarity, was measured and is plotted in Figure 11 vs $[SDS]^{1/4}$. Konuk et al.[43] reported a III/I ratio of 0.99 for SDS at a concentration near 100 mM, so these results compare well with the literature. The variation is small and the scatter is large; nevertheless, the trend is the same as that measured with EPR: namely, the probe-sensed polarity decreases with micelle size.

Comparing Figure 11 with Figure 2 of ref 13 shows that the EPR method offers far more precision in detecting micelle changes from measured polarity variations.

Conclusions

SDS micelles grow as the one-fourth power of the detergent concentration independent of detergents' source and independent of the quencher distribution function used to reduce the data. A small electrostatic interaction, of the same order of magnitude found in EPR experiments,[9,17] improves the fit of the theory to the aggregation number vs Cu^{2+} concentration. The quenching constants due to Cu^{2+} decrease as the micelle sizes increase in a manner consistent with diffusional encounters near the suface of the micelle with diffusion coefficents of the same order of magnitude as in water. Pyrene is readily available at the micelle surface and the residence time of the Cu^{2+} upon any given head group must be rather short.

Acknowledgment. This work was supported by a grant from the Royal Academy of Arts and Sciences of Uppsala. We gratefully acknowledge the contribution of Göran Svensk, who carried out the drop volume surface tension measurements. It is with sincere pleasure that B.L.B. acknowledges the patient guidance, instruction, and help of Cecilia Lindblad.

Appendix A. Single Curve Uncertainties

The nonlinear least-squares fit of eq 3 to an experimental decay curve yields estimates of the parameters in eqs 5−8; A_j, $j = 1-4$. The uncertainties in these quantities derived from the covariance matrix, denoted δA_j, are only estimates since there are significant cross correlations in the parameters. Defining the parameter $\phi = (A_2 - k_0)/A_3A_4$, the quantities of interest are computed from the following:

$$k_q = A_4/(1 + \phi) \tag{29}$$

$$k_- = \phi k_q \tag{30}$$

$$\langle N\rangle = A_3(1 + \phi)^2 \tag{31}$$

According to eq 30, ϕ is a measure of the relative importance of the migration rate, k_-, of the Cu^{2+} ions to their quenching rate, k_q. In these experiments, ϕ reaches a maximum of about 10% at [SDS] = 200 mM and maximum values of η (Figure 7). To estimate the uncertainties in the derived quantities, we treat the A_j as if they *were* independent and compute, for example

$$(\delta k_q)^2 = \sum_{j=2}^{4}\left[\frac{\partial k_q}{\partial A_j}\delta A_j\right]^2 \tag{32}$$

and two analogous expressions for δk_-, and $\delta\langle N\rangle$. The results

are as follows:

$$\left(\frac{\delta k_q}{k_q}\right)^2 = \left\{\left[\frac{1}{A_3A_4}\frac{1}{(1+\phi)}\delta A_2\right]^2 + \left[\frac{1}{A_3}\frac{\phi}{(1+\phi)}\delta A_3\right]^2 + \left[\frac{1}{A_4}\frac{(1+2\phi)}{(1+\phi)}\delta A_4\right]^2\right\} \quad (33)$$

$$\left(\frac{\delta k_-}{k_q}\right)^2 = \left\{\left[\frac{1}{A_3A_4}\frac{1}{(1+\phi)}\delta A_2\right]^2 + \left[\frac{1}{A_3}\frac{\phi}{(1+\phi)}\delta A_3\right]^2 + \left[\frac{1}{A_4}\frac{\phi}{(1+\phi)}\delta A_4\right]^2\right\} \quad (34)$$

$$\left(\frac{\delta\langle N\rangle}{\langle N\rangle}\right)^2 = \left\{\left[\frac{2}{A_3A_4}\frac{1}{(1+\phi)}\delta A_2\right]^2 + \left[\frac{1}{A_3}\frac{(1-\phi)}{(1+\phi)}\delta A_3\right]^2 + \left[\frac{1}{A_4}\frac{2\phi}{(1+\phi)}\delta A_4\right]^2\right\} \quad (35)$$

For small ϕ, that is, for small [SDS] and small η, the relative uncertainties of k_q and $\langle N\rangle$ are dominated by the relative uncertainties of A_4 and A_3, respectively. As [SDS] is increased from 25 to 200 mM, ϕ increases and other terms in eqs 31 and 33 contribute. In eq 33, the first term contributes less than 1% and the second term less than 4% at all values of ϕ. In eq 35, the first and third terms contribute 5−10% for [SDS] = 25−100 mM and become comparable to the second term at [SDS] = 200 mM.

References and Notes

(1) Fendler, J. H.; Fendler, E. H. *Catalysis in Micellar and Macromolecular Systems*; Academic Press: New York, 1975.
(2) Fendler, J. H. *J. Phys. Chem.* **1985**, *89*, 2730.
(3) Tachiya, M. In *Kinetics of Nonhomogeneous Processes*; Freeman, G. R., Ed.; John Wiley and Sons: New York, 1987; p 576.
(4) Bunton, C. A.; Nome, F.; Quina, F. H.; Romsted, L. S. *Acc. Chem. Res.* **1991**, *24*, 357.
(5) Gehlen, M. H.; De Schryver, F. C. *Chem. Rev.* **1993**, *93*, 199.
(6) Almgren, M. In *Kinetics and Catalysis in Microheterogeneous Systems*; Marcel Dekker: New York, 1991; p 63.
(7) Grieser, F.; Drummond, C. J. *J. Phys. Chem.* **1988**, *92*, 5580.
(8) Aizawa, M. *J. Phys. Chem.* **1992**, *96*, 3902.
(9) Bales, B. L.; Stenland, C. *J. Phys. Chem.* **1993**, *97*, 3418.
(10) Sankaram, M. B.; Marsh, D.; Thompson, T. E. *Biophys. J.* **1992**, *63*, 340.
(11) Shirahama, K.; Tohdo, M.; Murahashi, M. *Colloid Polym. Sci.* **1984**, *262*, 978.
(12) Yamaguchi, T.; Yamauchi, A.; Kimoto, E.; Kimizuka, H. *Bull. Chem. Soc. Jpn.* **1986**, *59*, 3029.
(13) Bales, B. L.; Stenland, C. *Chem. Phys. Lett.* **1992**, *200*, 475.
(14) Croonen, Y.; Geladé, E.; Van der Zegel, M.; Van der Auweraer, M.; Vandendriessche, H.; De Schryver, F. C.; Almgren, M. *J. Phys. Chem.* **1983**, *87*, 1426.
(15) Bezzobotnov, V. Y.; Borbely, S.; Cser, L.; Farago, B.; Gladkih, I. A.; Ostanevich, Y. M. *J. Phys. Chem.* **1988**, *92*, 5738.
(16) Van der Auweraer, M.; Dederen, J.; Geladé, E.; De Schryver, F. C. *J. Chem. Phys.* **1981**, *74*, 1140.
(17) Bales, B. L.; Stenland, C. *J. Phys. Chem.* **1995**, *99*, 15163.
(18) Infelta, P. P.; Grätzel, M.; Thomas, J. K. *J. Phys. Chem.* **1974**, *78*, 190.
(19) Tachiya, M. *Chem. Phys. Lett.* **1975**, *33*, 289.
(20) Miller, D. J. *Colloid Polym. Sci.* **1989**, *267*, 929.
(21) Tornberg, E. *J. Colloid Interface Sci.* **1977**, *60*, 50.
(22) Wilkinson, W. C. *J. Colloid Interface Sci.* **1972**, *40*, 14.
(23) Sasaki, T.; Hattori, M.; Sasaki, J.; Nukina, K. *Bull. Chem. Soc. Jpn.* **1975**, *48*, 1397.
(24) Doughty, D. A. *J. Phys. Chem.* **1979**, *83*, 2621.
(25) Almgren, M.; Hansson, P.; Mukhtar, E.; van Stam, J. *Langmuir* **1992**, *8*, 2405.
(26) Medhage, B.; Almgren, M.; Alsins, J. *J. Phys. Chem.* **1993**, *97*, 7753.
(27) Almgren, M.; Linse, P.; Van der Auweraer, M.; De Schryver, F. C.; Geladé, E.; Croonen, Y. *J. Phys. Chem.* **1984**, *88*, 289.
(28) Almgren, M. *Adv. Colloid Interface Sci.* **1992**, *41*, 9.
(29) Siemiarczuk, A.; Ware, W. R.; Liu, Y. S. *J. Phys. Chem.* **1993**, *97*, 8082.
(30) Luo, H.; Boens, N.; Van der Auweraer, M.; De Schryver, F. C.; Malliaris, A. *J. Phys. Chem.* **1989**, *93*, 3244.
(31) Dederen, J. C.; Van der Auweraer, M.; De Schryver, F. C. *J. Phys. Chem.* **1981**, *85*, 1198.
(32) Grieser, F.; Tausch-Treml, R. *J. Am. Chem. Soc.* **1980**, *102*, 7258.
(33) Nakamura, T.; Kira, A.; Imamura, M. *J. Phys. Chem.* **1983**, *87*, 3122.
(34) Almgren, M.; Löfroth, J. *J. Colloid Interface Sci.* **1981**, *81*, 486.
(35) Malliaric, A.; Lang, J.; Zana, R. *J. Chem. Soc., Faraday Trans. 1* **1981**, *82*, 109.
(36) Kratohvil, J. P. *J. Colloid Interface Sci.* **1980**, *75*, 271.
(37) Huisman, H. F. *Proc. Kon. Ned. Akad. Wetensch.* **1964**, *B67*, 367.
(38) Hall, D. G.; Pethica, B. A. In *Non-ionic Surfactants*; Schick, M., Ed.; Marcel Dekker: New York, 1967;
(39) Nagarajan, R. *Langmuir* **1994**, *10*, 2028.
(40) Aniasson, E. A. G.; Wall, S. N.; Almgren, M.; Hoffman, H.; Kielmann, I.; Ulbricht, W.; Zana, R.; Lang, J.; Tondre, C. *J. Phys. Chem.* **1976**, *80*, 905.
(41) Knauer, B. R.; Napier, J. J. *J. Am. Chem. Soc.* **1976**, *98*, 4395.
(42) Reddock, A. H.; Konishi, S. *J. Chem. Phys.* **1979**, *70*, 2121.
(43) Konuk, R.; Cornelisse, J.; McGlynn, S. P. *J. Phys. Chem.* **1989**, *93*, 7405.

JP9508665